Detection and global quantification of cardiovascular molecular calcification by fluoro-18-fluoride positron emission tomography/computed tomography-A novel concept

Mohsen Beheshti[1] MD,
Babak Saboury[2] MD, MPH,
Nehal N. Mehta[3,4] MD, MS
Drew A. Torigian[2] MD, MA,
Tom Werner[2] BA,
Emile Mohler[3] MD, MS,
Robert Wilensky[3] MD,
Andrew B. Newberg[5] MD,
Sandip Basu[6] MBBS(Hons)
DRM, DNB, MNAMS,
Werner Langsteger[1] MD,
Abass Alavi[2] MD, MD (Hon),
PhD (Hon), DSc (Hon)

1. Department of Nuclear Medicine and Endocrinology, PET/CT Center, St. Vincent's Hospital, Linz, Austria
2. Department of Radiology and
3. Penn Cardiovascular Institute
4. Center for Clinical Epidemiology and Biostatistics, University of Pennsylvania School of Medicine, Philadelphia, PA, USA
5. Department of Radiology, Thomas Jefferson University, Philadelphia, PA, USA
6. Radiation Medicine Centre (B.A.R.C),Tata Memorial Centre Annexe, Jerbai Wadia Road, Parel, Mumbai 400012, India

***

Keywords: Atherosclerosis
- Molecular calcification
- Fluoride PET/CT
- Global quantification

Correspondence address:
Abass Alavi, MD. Department of Radiology, Hospital of the University of Pennsylvania, 3400 Spruce Street, Philadelphia, PA 19104, USA, Phone: 215-662-3069, Fax: 215-573-4107., E-mail: abass.alavi@uphs.upenn.edu

Received:
    10 June 2011
Accepted:
    16 June 2011

Abstract

The aim of this study was to examine the degree and prevalence of regional (aorta) and global (cardiac) fluorine-18-sodium fluoride (^{18}F-NaF) uptake by positron emission tomography (PET) – computed tomography (CT) as evidence for calcification in the atherosclerotic plaques in the aorta and the heart as a function of age. *Image data* from 51 patients, who had undergone whole-body ^{18}F-Na FPET/CT, were evaluated retrospectively. Cardiac and arterial (aorta) radiotracer uptakes were analyzed quantitatively by measuring standard uptake values (SUV). This approach involved examining the entire heart and various aortic segments as identified by CT. By combining CT and PET data, regional and global concentrations of this molecule were calculated and correlated with age over the decades. ^{18}F-NaF uptake in the heart and aorta increased significantly with advancing age (P <0.01). The Pearson correlation coefficient for the mean ^{18}F-NaF uptake of cardiac region and 5 age groups was 0.92 (P=0.003) and for aorta and 5 age groups was 0.97 (P=0.004). *In conclusion,* these preliminary data indicate the feasibility of ^{18}F-NaF-PET/CT for measurement of regional and global calcification of the heart and major arteries. The ^{18}F-NaF-PET/CT may provide highly relevant information about the state of calcified plaque before structural calcification is detectable by standard CT techniques. This, therefore, may allow for earlier intervention for risk reduction in cardiovascular diseases. Further studies are needed to validate the role of this promising technique in the management of patients with suspected atherosclerosis.

Introduction

Atherosclerosis and coronary heart disease (CHD) are the main causes of major morbidities and mortality in Western societies despite aggressive preventive strategies [1]. Atherosclerosis usually starts in the early decades of life and develops over the ensuing years, while often remaining asymptomatic until an acute life threatening event occurs during the course of the disease [2]. Furthermore, over half of acute myocardial infarctions or sudden cardiac death events occur in previously asymptomatic individuals [3]. Thus, there is a continued search for optimal biomarkers to allow for early and accurate identification of individuals at risk for this potentially fatal disease and subsequent implementation of timely interventions to modulate the atherosclerotic process.

Clinically, early detection of atherosclerosis should lead to initiating appropriate intervention before significant disease occurs, therefore, preventing serious complications in the future [4]. For this reason, the in vivo study of the atherosclerotic *process,* rather than its risk factors, will enable accurate and early identification of high risk individuals.

Although studies of coronary artery calcification(CAC) [5-7] and intimal medial thickness (IMT) [8, 9] have clinical utility for predicting future events, uncertainty [10, 11] among those without positive findings still exists [12]. These modalities do not accurately assess plaque characteristics [12, 13], including the composition and inflammatory state of plaqueas well as the degree of molecular calcification which reflects plaque stability and, therefore, the risk of future clinical events [14-18]. Given the need for the development and validation of imaging techniques to allow for early detection and quantification of molecular changes in atherosclerotic plaque, we sought to assess whether imaging uptake of fluorine-18-sodium fluoride (^{18}F-NaF) would be successful in detecting the process of molecular calcification in the vasculature. If ^{18}F-NaF positron emission tomography (PET) imaging is successful in detecting cardiovascular calcifications, this may allow early intervention in the disease course and prior to overt calcification seen on computed tomography (CT). Since the degree of uptake of this radiotracer in the heart and major vessels is low, therefore visual detection of its presence and regional quantification of its concentration are suboptimal for the early assessment of this process. We introduce a new concept for calculating

global calcification as a sensitive biomarker for detection of early molecular and cellular calcification in the atherosclerotic plaques. The results of this retrospective work based upon this novel premise form the basis for undertaking well planned prospective studies in the future. Thus, the purpose of this initial study was to assess the prevalence, location, and relationship of increased ^{18}F-NaF uptake in the heart and aortic wall with normal aging as demonstrated by PET/CT as evidence for molecular calcification.

Methods

Patients

This study was approved by the local Institutional Review Board. In this retrospective study we examined the image data sets of 51 patients who had undergone ^{18}F-NaF-PET/CT for evaluation of a variety of malignancies. The exclusion criteria included history of recent myocardial infarction, cardiomyopathy, pericarditis, myocarditis, recent radiotherapy to the thorax (within 3 months), amyloidosis, renal insufficiency, and active mediastinal bulky disease (e.g. lymphoma, granulomatous disease).

The mean age of patients was 63 years, ranging from 29-90 years. Seventeen (33%) were males, and 34 (66%) were females. Nineteen patients (37%) were ≤ 60 years old and 32 (63%) were >60 years old. Subjects were categorized into five age-groups: ≤40, 41-50, 51-60, 61-70 and >70 years old (Table 1).

Table 1. *Age and gender demographics features of the study population*

Age Group	Male	Female	Total
≤40	1	1	2
41-50	2	5	7
51-60	3	7	10
61-70	5	15	20
>70	5	6	11

PET/CT imaging

Imaging was performed on an integrated PET/CT system (Discovery LS , GE Medical Systems, Milwaukee, WI) that consisted of a full-ring PET scanner with a 14.6cm transverse axial field of view and an in- plane spatial resolution of 4.8mm full width at half maximum at the center of the field and a four slice CT scanner. All PET scans were acquired in 2D mode (4min emission per bed position) and were reconstructed with standard reconstruction ordered-subset expectation maximization iterative algorithm (two iterative steps) and were reformatted into transverse, coronal, and sagittal views. Radiochemical synthesis and the characteristics of ^{18}F-NaF (IASOflu) have been described in the literature by Nader et al (2007) [19].

[18]F-NaF-PET/CT acquisition was started 60min after intravenous injection of 370-550MBq of the compound and included 12-13 bed positions for a whole body scan. An unenhanced CT was performed for anatomic localization and attenuation correction (140kV, 0.5sec per rotation, 5.0mm reconstructed section thickness, 0.5mm overlap) with a low beam current modulation (80- 120mA).

Image interpretation and quantitative data analysis

Positron emission tomography scans were analyzed by an experienced nuclear medicine physician who was not aware of the clinical parameters or findings of the patients examined. Images were read and analyzed sequentially using an advanced PET/CT review software (Advantage Windows 4.2–7, GE Medical Systems, Milwaukee, WI), which allows simultaneous scrolling through the corresponding PET, CT, and fusion images in transverse, coronal, and sagittal planes.

An ellipsoid region of interest (ROI) was drawn on each CT image around the ventricles on transverse slices (Fig. 1).The aortic valve was excluded from ROI to avoid contamination by the aortic wall or calcified aortic valve leaflets which might interfere with this analysis. Regions of interest were placed on all transverse images from the base to the apex of the heart with a fixed CT slice thickness of 4.5mm, and were then transferred to corresponding transverse PET images. Then, the volume of each slice was calculated by multiplying the area on the ROI by the slice thickness. Quantitative analysis of PET images was then performed by generating mean standardized uptake value (SUVmean) of each ROI.
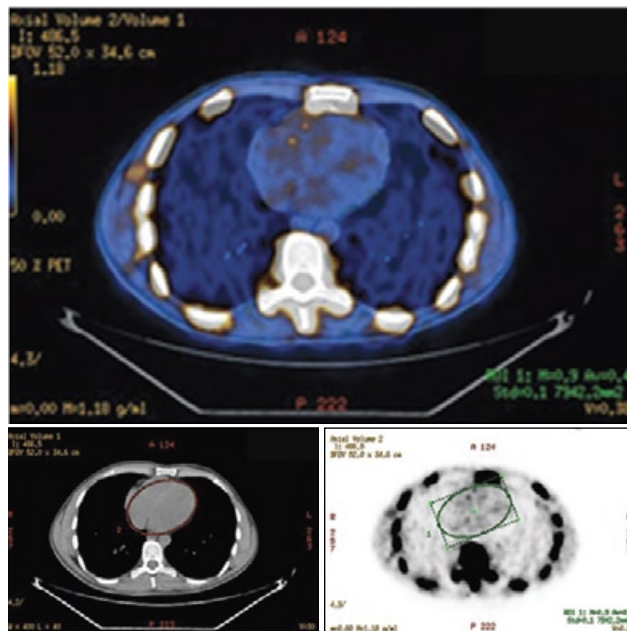

Figure 1. This figure demonstrates a typical region of interest (ROI) that was assigned to the cardiac silhouette on each slices of CT and the corresponding PET slice. As noted above, the degree of ^{18}F-Na Fuptake is quite non-uniform throughout the selected slice and thus, is of limited value for accurate assessment of related calcification. Also, please note that the process of uptake is diffused and does not conform to the shape of the ventricles lumen in either ventricles. In this particular slice the volume of the selected ROI was 30.8 cc, and the SUVmean on the corresponding PET slice was 0.5. Therefore, the molecular calcification score for this particular slice was calculated to be 15.4 (30.8x0.5 = 15.4). The Global Calcification Score for the entire heart was calculated by adding the individual slice values generated by this approach.

The cardiac Global Molecular Calcification Score (GMCS) for each patient was generated as follows: for each transverse slice, the ROI volume of the tissue examined was calculated by multiplying the area of the ROI by its slice thickness. Then, the ROI volumes determined by CT were multiplied by the SUVmean generated from the same ROI assigned to

calculate the molecular calcification score in that particular slice. Finally, the cardiac GMCS was generated by summing the molecular calcification scores among the entire set of ROI analyzed.

For analysis of the aorta, fixed cylindrical volumes of interest (VOI) (with dimensions 20x20x30mm) were placed using transverse, coronal, and sagittal CT images for anatomic guidance. One VOI was placed over the lower thoracic aorta between the T4-T8 vertebral levels, and another VOI was placed over the abdominal aorta between the T12-L4 vertebral levels depending on the anatomic configuration of the aorta among different patients. Volumes of interest were then transferred to corresponding PET images. The SUVmean of the two VOI was recorded and averaged to generate aortic SUVmean as a measure of aortic molecular calcification.

Statistical analysis

Analysis was performed using the Stata 11 (StataCorp. 2009. *Stata Statistical Software: Release 11*. College Station, TX: StataCorp LP). An unpairedest test was performed to assess for statistically significant differences in mean cardiac GMCS and aortic SUVmean for patients ≤ 60 vs. >60 years of age. Subjects were also categorized in predefined age groups (≤ 40 year, 41-50, 51-60, 61-70, >70) where results for each age group from PET/CT analysis were reported as mean ($\pm$standard deviation (SD)). Correlational analyses between mean cardiac GMCS and age group and between the mean of aortic SUVmean and age group were then performed to calculate Pearson correlation coefficients. We also evaluated whether renal function affects the GMCS to ensure that renal function changes would not influence the findings. To examine the effect of creatinine level on GMCS we categorized our subjects into four groups (by age (<=60, >60) and creatinine level (<=predicted creatinine level (Hi), >predicted creatinine level (Low)).

By fitting regression models on the creatinine and age, we calculated predicted creatinine level of each subject based on their age. And then classified that subject into two categories of "Hi creatinine level", if the measured creatinine level was higher than predicted value and of "Low creatinine level", if the measured creatinine level was lower than predicted value. A t-test was performed to determine if there were differences between these groups with respect to GMCS.

P-values <0.05 were considered as statistically significant for all statistical analyses performed.

Results

Cardiac GMCS

The mean ($\pm$SD) of cardiac GMCS of each age group is presented in Table 2. The Pearson correlation coefficient for correlation between mean cardiac GMCS and the 5 age groups was 0.92 (P=0.003) (Fig. 2). The mean ($\pm$SD) of cardiac GMCS in patients ≤ 60 years of age was 25.6$\pm$2 whereas that in patients >60 years was 34.5$\pm$3 (P=0.04).

In younger subjects (age<=60), the GMCS of "Hi creatinine" and "Low creatinine" groups were 38.63$\pm$9.37 and 28.86$\pm$5.84 respectively. And this difference was not statistically significant (P-value=0.43). Also in older subjects (Age>60) the GMCS of "Hi creatinine" and "Low creatinine" groups were

Table 2. *Cardiac Global Molecular Calcification Score*

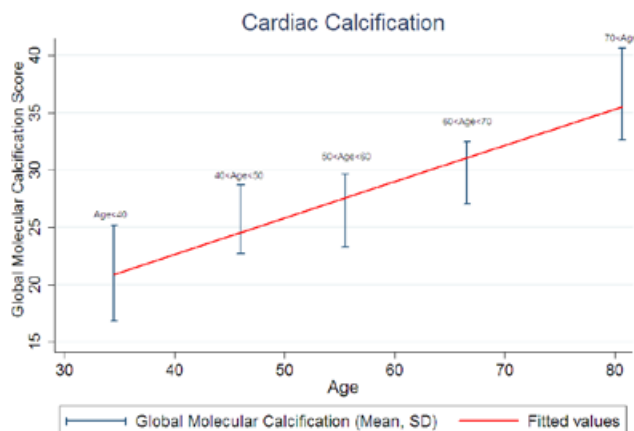| Age Group	GMCS: mean($\pm$SD)
≤ 40	21.00 $\pm$ 4.20
41-50	25.71 $\pm$ 2.98
51-60	26.46 $\pm$ 3.19
61-70	29.76 $\pm$ 2.71
>70	36.65 $\pm$ 4.00

Figure 2. Relationship between cardiac Global Molecular Calcification Score (GMCS), as measured by ^{18}F-NaF-PET/CT and age. The GMCS data points (mean and SD) reflect ^{18}F-NaF uptake in 5 different age groups as shown above. The fitted line shows a statistically significant increase in cardiac molecular calcification with age (Pearson correlation coefficient = 0.92; P=0.003).

30.8$\pm$2.38 and 32.36$\pm$4.86, respectively, and this difference was not statistically significant (P-value=0.80). In conclusion, the creatinine level was not considered as a confounder factor in the relation of GMCS and age, since there was no statistically significant relation between creatinine and GMCS. Therefore, blood pool activity as a contaminant for calculating myocardial uptake of ^{18}F was thought to be negligible. Also, the appearance of the signals detected from the heart region did not conform to the typical ventricular cavities and was quite irregular in appearance (Fig. 1).

Aortic molecular calcification

The mean $\pm$SD of aortic SUVmean of each age group is presented in Table 3. The Pearson correlation coefficient for correlation between the mean of aortic SUVmean and the 5 age groups was 0.97 (P=0.004) (Fig. 3). The mean ($\pm$SD) of aortic SUVmean in patients ≤ 60 years was 0.83($\pm$0.04) whereas that in patients >60 years was 0.99$\pm$0.03 (P=0.004).The Pearson correlation coefficient between mean cardiac GMCS and aortic SUVmean measurements in each subject was 0.57 (P< 0.01).

Table 3. *Aortic SUVmean on ^{18}F-NaF PET/CT*

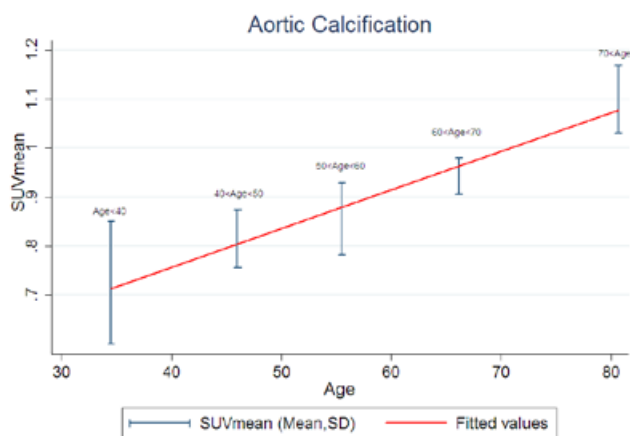| Age Group	SUVmean: mean($\pm$SD)
≤ 40	0.72 $\pm$ 0.12
41-50	0.81 $\pm$ 0.06
51-60	0.86 $\pm$ 0.07
61-70	0.94 $\pm$ 0.03
>70	1.10 $\pm$ 0.06

Figure 3: Relationship between aortic SUVmean, as measured by ^{18}F-NaF-PET/CT, and age. The aortic SUVmean data points (mean and SD) reflect ^{18}F-NaF uptake in 5 different age groups as shown above. The fitted line shows a statistically significant increase in aortic molecular calcification with age (Pearson correlation coefficient =0.97; P=0.004).

In general, minimal if any calcification was noted in the cardiac region on CT images. Some patients were noted to have calcifications in the aorta. Please note that we did not quantify the extent and degree of calcification on CT during this study. Of note, CT scanning was performed for attenuation and localization (of the PET findings) purposes. Conventional calcium scoring on CT requires high resolution gated imaging which was not available for these subjects. On ^{18}F-NaF-PET images, no discrete or localized foci of radiotracer uptake were noted either in the cardiac region or aorta. As noted above, on the visual inspection, radiotracer uptake in the heart was diffuse but minimally perceptible.

Discussion

The results from this initial study demonstrate the potential feasibility of using ^{18}F-NaF-PET/CT for in vivo quantification of molecular calcification in the heart and aorta, as an early feature of atherosclerosis in the evolution of its course. The finding that the degree of both cardiac and aortic calcification correlates significantly with age validates the theoretical notion that age is associated with the degree and extent of calcification. Therefore, this modality is potentially applicable to the management of patients with suspected atherosclerosis. Although preliminary in nature, our data show the first proof of concept for this technique and reveal that age, the most potent cardiovascular risk factor, is highly correlated with the degree of molecular calcification in the heart and aorta. These early results also provide approximate normal values and standard deviation for the GMCS which can be useful for future studies, particularly in patients at high risk for developing atherosclerosis.

The introduction of PET as a powerful clinical and research tool has rejuvenated interest for its utilization with[18]F-NaF for assessment of osseous structures as well as early detection of calcification in the soft tissue [20, 21]. In particular, the significant shortage of technetium-99m (^{99m}Tc) for labeling a variety of compounds, and the greater availability, superior spatial and contrast resolutions, and potential for accurate quantification of PET and PET/CT compared with SPET and

planar scintigraphy, prompted us to undertake this investigation. A large number of papers have been published in the literature that describe the utility of ^{18}F-NaF-PET or PET/CT to assess malignant [22-25] and benign disorders of the skeletal system [26-28]. However, due to minimal uptake of either ^{99m}Tc labeled compounds or ^{18}F in the heart and the aorta as an evidence for molecular calcification has resulted in overlooking by this very important phenomenon on planar scintigraphy and single photon emission tomography (SPET). Therefore, no attempt has been made to pursue the significance of this observation in both normal and pathologic states. This is particularly true when regional measurements, typically via placement of a single 2D ROI, are performed, which in this scenario tend to provide statistically insignificant data due to low signal to noise ratios. In contrast, the statistical reliability of this type of analysis can substantially improve by utilizing a global approach for disease evaluation as has been shown in other domains [29, 30].

The major reason for this initiating research study was to determine whether global measures of ^{18}F-NaF uptake in the heart and aorta could be of value in detecting and quantifying molecular calcification in these structures and to assess the cause of atherosclerotic process. Our work extends the work of Derlin et al (2010) [31], who reported the feasibility of ^{18}F-NaF-PET to image calcium deposition in the arterial wall as visualized by CT. The results from our study indicate that even without visible calcification in the heart and aorta, there is evidence for ongoing molecular calcification, which opens up a new avenue of research in atherosclerosis and effective management of this disorder. Global quantitative assessment of molecular calcification in the heart and aorta provides a novel and practical method of studying the course of atherosclerosis, to risk stratify patients with regard to clinical outcome early in the disease course, and to objectively monitor the effects of therapeutic interventions at various stages of this serious disorder.

Arterial calcification has been studied mainly through electron beam computed tomography (EBCT) [32] and multi-detector row computed tomography (MDCT) technologies, which are structural imaging techniques that are likely to provide limited functional or molecular characterization of atherosclerotic plaque [11]. These modalities detect structural macroscopic calcification, thereby providing information about atherosclerotic damage which has already occurred over the ensuing years [33, 34]. Also, there is presently a gap and controversy in the understanding of how CT imaging characteristics of atherosclerosis precisely relate to the natural history of atherosclerotic plaque [35-38, 16]. Furthermore, conventional CT imaging for this purpose is associated with significant radiation dose to the patient which is becoming a major source of concern in medicine.

Thus, the utilization of[18]F-NaF-PET/CT imaging may be useful to bridge this gap, between cellular inflammation as detected by ^{18}F-FDG-PET [39, 40] and CT calcification stage. It is conceivable that molecular calcification detected by[18]F-NaF-PET/CT at earlier stages of the atherosclerotic process will allow for appropriate therapeutic intervention when the process is more likely to be reversible (Fig. 4). Microcalcification has been implicated in plaque rupture [41], and the ability of ^{18}F-NaF-PET/CT to provide information about both plaque function and structure in a single examination allows for its potential use in the risk stratification and treatment of

patients with atherosclerosis. This is possible since the[18]F[-] ion exchanges with the hydroxyl group at the sites of molecular calcification, and a high degree of correlation been reported between the presence of calcification and the uptake of ^{18}F-NaF on PET images [21]. It can be foreseen, that ^{18}F-NaF-PET/CT can potentially provide information about different atherosclerotic phenotypes and associated probabilities of future cardiovascular events, which can then be modulated in the short- and long-terms with therapeutic interventions [42, 43, 14, 44].
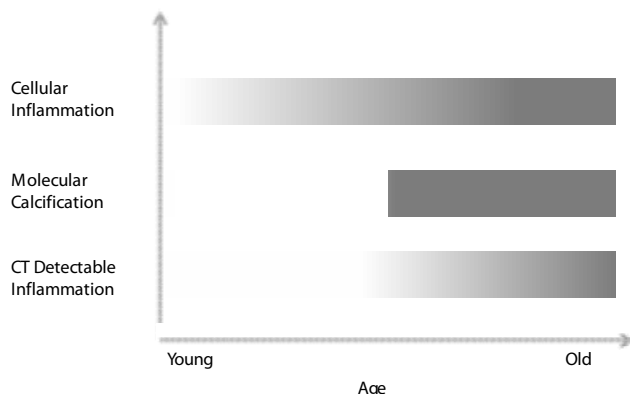

Figure 4. The graph above depicts our hypothesis about the sequences of events with regard to atherogenesis and its evolution over time. Inflammatory lesions related to atherosclerosis marks the beginning of this process and are followed by molecular calcification years later. Molecular and cellular imaging with PET will allow detection and quantification of these processes soon after they are initiated. However, if untreated molecular calcification eventually will lead to structural calcification that can be diagnosed by structural imaging modalities such as CT.

The main limitations of this study are the lack of available information about the medication history of subjects included, the retrospective and cross-sectional design, the lack of histopathological or clinical outcome data, and the single center nature of this study. However, the data generated support the hypotheses underlying this investigation. Based on these results we propose a novel scheme (Fig. 4) that may elucidate the time course of atherosclerotic disorders and the relevance of modern imaging modalities at different phases of the underlying processes.

An important difference between[18]F-NaF and ^{99m}Tc-diphosphonate bone agents is minimal binding of the former with serum proteins which is substantial for the latter binding. Approximately 30% of ^{99m}Tc-MDP is protein-bound immediately after injection; this fraction increases to approximately 70% by 24h after injection [45-47]. The protein-bound fraction is cleared much more slowly compared to the non protein bound fraction. The first phase of ^{18}F-fluoride clearance from plasma, where the [18]F[-] ion exchanges for an OH^{-} ion on the surface of the hydroxyapatite matrix of bone has a half-life of 0.4h, whereas the second phase, where the [18]F[-] ion migrates into the crystalline matrix of bone and retained there till the bone is remodelled has a half-life of 2.6h [48, 49]. This indicates that almost the entire compound is cleared from the circulation by 60min. Therefore, it is necessary to wait 3-4h after injection of ^{99m}Tc-MDP before imaging while, the rapid uptake in bone and fast clearance from soft tissue of ^{18}F-fluorideallows data recording to commence no later than one hour after intravenous administration of NaF. It is estimated that around 1h after administration of ^{18}F-labeled NaF, a small fraction of the injected dose remains in the blood [50]. Because of the nature of this retrospective analysis, where images were acquired 1h after injection the effect of delayed imaging could not be determined. Efforts are underway to determine the optimal timing for this purpose and establish a standard protocol.

Molecular calcification as assessed by ^{18}F-NaF likely will provide highly relevant information to our understanding of this common disorder before structural calcification is detectable by standard CT techniques. This, we believe, will add a new dimension to FDG-PET imaging, which is being actively investigated in the assessment of atherosclewsis [51]. We therefore hypothesize that ^{18}F-NaF-PET/CT imaging may allow for accurate early risk stratification and therapeutic intervention in patients with atherosclerosis through this very powerful quantitative technique. However, a large scale prospective study is required to test this hypothesis.

These preliminary results clearly demonstrate the need for a larger scale prospective research study to validate the potential role of this approach for comprehensive quantitative assessment of underlying processes that are related to molecular aspect of atherosclerosis in the cardiovascular system.

In conclusion, our data provide evidence for feasibility of ^{18}F-NaF-PET/CT for quantification of global molecular calcification of the heart and aorta, and by demonstrating statistically significant correlation between the uptake of the uptake in the heart and aorta with increasing age. Fluorine-18-NaF-PET/CT may therefore provide highly relevant information about the properties of calcified plaque long before macroscopic calcification will be detectable by CT, potentially allowing for earlier risk stratification and therapeutic intervention in a timely manner in patients with asymptomatic atherosclerosis.

The authors declare that they have no conflicts of interest.

Bibliography

1. Helfand M, Buckley DI, Freeman M et al. Emerging risk factors for coronary heart disease: a summary of systematic reviews conducted for the U.S. Preventive Services Task Force. *Ann Intern Med* 2009; 151(7): 496-507. doi:151/7/496 [pii].

2. Libby P. Inflammation in atherosclerosis. *Nature* 2002; 420(6917): 868-74.

3. Smith SC, Jr., Allen J, Blair SN et al. AHA/ACC guidelines for secondary prevention for patients with coronary and other atherosclerotic vascular disease: 2006 update: endorsed by the National Heart, Lung, and Blood Institute. *Circulation* 2006; 113(19): 2363-72.

4. Greenland P, Knoll MD, Stamler J et al. Major risk factors as antecedents of fatal and nonfatal coronary heart disease events. *Jama* 2003; 290(7): 891-7.

5. Detrano R, Guerci AD, Carr JJ et al. Coronary calcium as a predictor of coronary events in four racial or ethnic groups. *N Engl J Med* 2008; 358(13): 1336-45. doi:358/13/1336 [pii] 10.1056/NEJMoa072100.

6. Raggi P, Cooil B, Ratti C et al. Progression of Coronary Artery Calcium and Occurrence of Myocardial Infarction in Patients With and Without Diabetes Mellitus. *Hypertension* 2005; 46(1): 238-43.

7. Arad Y, Goodman KJ, Roth M et al. Coronary calcification, coronary disease risk factors, C-reactive protein, and atherosclerotic cardiovascular disease events: the St. Francis Heart Study. *J Am Coll Cardiol* 2005; 46(1): 158-65.

8. Lorenz MW, Markus HS, Bots ML et al. Prediction of clinical cardiovascular events with carotid intima-media thickness: a systematic review and meta-analysis. *Circulation* 2007; 115(4): 459-67. doi:CIRCULATION AHA.106.628875 [pii] 10.1161/CIRCU LATIONAHA.106.628875.

9. Kathiresan S, Larson MG, Keyes MJ et al. Assessment by cardiovascular magnetic resonance, electron beam computed tomography, and carotid ultrasonography of the distribution of subclinical atherosclerosis across Framingham risk strata. *Am J Cardiol* 2007; 99(3): 310-4. doi:S0002-9149(06)02053-4 [pii] 10.1016/j.amjcard.2006.08.028.

10. Bonow RO. Clinical practice. Should coronary calcium screening be used in cardiovascular prevention strategies? *N Engl J Med* 2009; 361(10): 990-7. doi:361/10/990 [pii] 10.1056/NEJMcp0902177.

11. Moser KW, O'Keefe JH, Jr., Bateman TM, McGhie IA. Coronary calcium screening in asymptomatic patients as a guide to risk factor modification and stress myocardial perfusion imaging. *J Nucl Cardiol* 2003; 10(6): 590-8.

12. Detrano RC, Wong ND, Doherty TM et al. Coronary calcium does not accurately predict near-term future coronary events in high-risk adults. *Circulation* 1999; 99(20): 2633-8.

13. Doherty TM, Detrano RC, Mautner SL et al. Coronary calcium: the good, the bad, and the uncertain. *Am Heart J* 1999; 137(5): 806-14.

14. Chen W, Bural GG, Torigian DA et al. Emerging role of FDG-PET/CT in assessing atherosclerosis in large arteries. *Eur J Nucl Med Mol Imaging* 2009; 36(1): 144-51. doi:10.1007/s00259-008-0947-2.

15. Doherty TM, Asotra K, Fitzpatrick LA et al. Calcification in atherosclerosis: bone biology and chronic inflammation at the arterial crossroads. *Proc Natl Acad Sci USA* 2003; 100(20): 11201-6. doi:10.1073/pnas.1932554100 1932554100 [pii].

16. Fuster V. Lewis A. Conner Memorial Lecture. Mechanisms leading to myocardial infarction: insights from studies of vascular biology. *Circulation* 1994; 90(4): 2126-46.

17. van der Wal AC, Becker AE, van der Loos CM et al. Fibrous and lipid-rich atherosclerotic plaques are part of interchangeable morphologies related to inflammation: a concept. *Coron Artery Dis* 1994; 5(6): 463-9.

18. van der Wal AC, Becker AE, van der Loos CM, Das PK. Site of intimal rupture or erosion of thrombosed coronary atherosclerotic plaques is characterized by an inflammatory process irrespective of the dominant plaque morphology. *Circulation* 1994; 89(1): 36-44.

19. Nader MW, Schubert M, DW B. Design and Validation of a semi-automated sodium [18F]fluoride formulation system. *J Nucl Med* 2007; 48(Suppl. 2): 136P.

20. Hoh CK, Hawkins RA, Dahlbom M et al. Whole body skeletal imaging with [18F]fluoride ion and PET. *J Comput Assist Tomogr* 1993; 17(1): 34-41.

21. Grant FD, Fahey FH, Packard AB et al. Skeletal PET with 18F-fluoride: applying new technology to an old tracer. *J Nucl Med* 2008; 49(1): 68-78. doi:jnumed.106.037200 [pii]10.2967/jnumed.106.037200.

22. Tse N, Hoh C, Hawkins R et al. Positron emission tomography diagnosis of pulmonary metastases in osteogenic sarcoma. *Am J Clin Oncol* 1994; 17(1): 22-5.

23. Schirrmeister H, Guhlmann A, Elsner K et al. Sensitivity in detecting osseous lesions depends on anatomic localization: planar bone scintigraphy versus 18F PET. *J Nucl Med* 1999; 40(10): 1623-9.

24. Schirrmeister H, Guhlmann A, Kotzerke J et al. Early detection and accurate description of extent of metastatic bone disease in breast cancer with fluoride ion and positron emission tomography. *J Clin Oncol* 1999; 17(8): 2381-9.

25. Beheshti M, Vali R, Waldenberger P et al. Detection of bone metastases in patients with prostate cancer by 18F fluorocholine and 18F fluoride PET-CT: a comparative study. *Eur J Nucl Med Mol Imaging* 2008; 35(10): 1766-74. doi:10.1007/s00259-008-0788-z.

26. Coady CM, Micheli LJ. Stress fractures in the pediatric athlete. *Clin Sports Med* 1997; 16(2): 225-38.

27. Ovadia D, Metser U, Lievshitz G et al. Back pain in adolescents: assessment with integrated 18F-fluoride positron-emission tomography-computed tomography. *J Pediatr Orthop* 2007; 27(1): 90-3. doi:10.1097/01.bpo.0000242438.11682.10 01241398-200701000-00017 [pii].

28. Lim R, Fahey FH, Drubach LA et al. Early experience with fluorine-18 sodium fluoride bone PET in young patients with back pain. *J Pediatr Orthop* 2007; 27(3): 277-82. doi:10.1097/BPO.0b013e31803409ba 01241398-200704000-00005 [pii].

29. Alavi A, Newberg AB, Souder E, Berlin JA. Quantitative analysis of PET and MRI data in normal aging and Alzheimer's disease: atrophy weighted total brain metabolism and absolute whole brain metabolism as reliable discriminators. *J Nucl Med* 1993; 34(10): 1681-7.

30. Basu S, Zaidi H, Houseni M et al. Novel quantitative techniques for assessing regional and global function and structure based on modern imaging modalities: implications for normal variation, aging and diseased states. *Semin Nucl Med* 2007; 37(3): 223-39. doi:S0001-2998(07)00021-9 [pii]10.1053/j.semnuclmed.2007.01.005.

31. Derlin T, Richter U, Bannas P et al. Feasibility of 18F-sodium fluoride PET/CT for imaging of atherosclerotic plaque. *J Nucl Med* 2010; 51(6): 862-5. doi:jnumed.110.076471 [pii]10.2967/jnumed.110.076471.

32. Rumberger JA, Simons DB, Fitzpatrick LA et al. Coronary artery calcium area by electron-beam computed tomography and coronary atherosclerotic plaque area. A histopathologic correlative study. *Circulation* 1995; 92(8): 2157-62.

33. Rumberger JA, Sheedy PF, 3rd, Breen JF, Schwartz RS. Coronary calcium, as determined by electron beam computed tomography, and coronary disease on arteriogram. Effect of patient's sex on diagnosis. *Circulation* 1995; 91(5): 1363-7.

34. Schmermund A, Denktas AE, Rumberger JA et al. Independent and incremental value of coronary artery calcium for predicting the extent of angiographic coronary artery disease: comparison with cardiac risk factors and radionuclide perfusion imaging. *J Am Coll Cardiol* 1999; 34(3): 777-86.

35. Corti R, Fuster V, Fayad ZA et al. Effects of aggressive versus conventional lipid-lowering therapy by simvastatin on human atherosclerotic lesions: a prospective, randomized, double-blind trial with high-resolution magnetic resonance imaging. *J Am Coll Cardiol* 2005; 46(1): 106-12.

36. Fayad ZA, Sirol M, Nikolaou K et al. Magnetic resonance imaging and computed tomography in assessment of atherosclerotic plaque. *Curr Atheroscler Rep* 2004; 6(3): 232-42.

37. Fuster V, Badimon L, Badimon JJ, Chesebro JH. The pathogenesis of coronary artery disease and the acute coronary syndromes (1). *N Engl J Med* 1992; 326(4): 242-50.

38. Zhang Z, Machac J, Helft G et al. Non-invasive imaging of atherosclerotic plaque macrophage in a rabbit model with 18F-FDG PET: a histopathological correlation. *BMC Nucl Med* 2006; 6: 3. doi:1471-2385-6-3 [pii] 10.1186/1471-2385-6-3.

39. Yun M, Jang S, Cucchiara A et al. [18]F FDG uptake in the large arteries: a correlation study with the atherogenic risk factors. *Semin Nucl Med* 2002; 32(1): 70-6. doi:S0001-2998(02)80041-1 [pii] 10.1053/snuc.2002.29279.

40. Yun M, Yeh D, Araujo LI et al. ^{18}F-FDG uptake in the large arteries: a new observation. *Clin Nucl Med* 2001; 26(4): 314-9.

41. Wilensky RL, Song HK, Ferrari VA. Role of magnetic resonance and intravascular magnetic resonance in the detection of vulnerable plaques. *J Am Coll Cardiol* 2006; 47(8 Suppl): C48-56. doi:S0735-1097(05)03141-4 [pii] 10.1016/j.jacc.2005.11.048.

42. Wasselius JA, Larsson SA, Jacobsson H. FDG-accumulating atherosclerotic plaques identified with ^{18}F-FDG-PET/CT in 141 patients. *Mol Imaging Biol* 2009; 11(6): 455-9. doi:10.1007/s11307-009-0223-2.

43. Mantovani A, Garlanda C, Locati M. Macrophage diversity and polarization in atherosclerosis: a question of balance. *Arterioscler Thromb Vasc Biol* 2009; 29(10): 1419-23. doi: ATVBAHA.108.180497 [pii] 10.1161/ATVBAHA.108.180497.

44. Tahara N, Kai H, Yamagishi S et al. Vascular inflammation evaluated by [^{18}F]-fluorodeoxyglucose positron emission tomography is associated with the metabolic syndrome. *J Am Coll Cardiol* 2007; 49(14): 1533-9.

45. Blake GM, Park-Holohan SJ, Cook GJ, Fogelman I. Quantitative studies of bone with the use of ^{18}F-fluoride and ^{99m}Tc-methylene diphosphonate. *Semin Nucl Med* 2001; 31(1): 28-49.

46. Chilton H, Francis M, Thrall J. Radiopharmaceuticals for bone and bone marrow imaging. In: Swanson D, Chilton H, Thrall J, editors. *Pharmaceuticals in Medical Imaging: Radiopaque Contrast Media, Radiopharmaceuticals, Enhancement Agents for Magnetic Resonance Imaging and Ultrasound.* New York, NY: Macmillan Pub. Co; 1990. p. 537-63.

47. Hyldstrup L, McNair P, Ring P, Henriksen O. Studies on diphosphonate kinetics. Part I: Evaluation of plasma elimination curves during 24h. *Eur J Nucl Med* 1987; 12(12): 581-4.

48. Costeas A, Woodard HQ, Laughlin JS. Depletion of ^{18}F from blood flowing through bone. *J Nucl Med* 1970; 11(1): 43-5.

49. Wootton R, Dore C. The single-passage extraction of ^{18}F in rabbit bone. *Clin Phys Physiol Meas* 1986; 7(4): 333-43.

50. Blau M, Ganatra R, Bender MA. ^{18}F-fluoride for bone imaging. *Semin Nucl Med* 1972; 2(1): 31-7.

51. SI. Bural GG. Torigich DA. Botvinick E etal. A pilot study of changes in ^{18}F-FDG uptake, calcification and global metabolic activity of the aorta with aging. *Hell Nucl Med* 2009; 12(2): 123-8.